

Research Article

Identification prognosis-associated immune genes in colon adenocarcinoma

Yandong Miao^{1,*}, Jiangtao Wang^{1,*}, Xueping Ma², Yuan Yang¹ and  Denghai Mi^{1,3}

¹The First Clinical Medical College of Lanzhou University, Lanzhou City, Gansu Province, P.R. China; ²Second People's Hospital of Gansu Province, Lanzhou City, Gansu Province, P.R. China; ³Gansu Academy of Traditional Chinese Medicine, Lanzhou City, Gansu Province, P.R. China

Correspondence: Denghai Mi (mi.dh@outlook.com)



Colon adenocarcinoma (COAD) is one of the most prevalent malignant tumors worldwide. Immune genes (IGs) have a considerable correlation with tumor initiation and prognosis. The present paper aims to identify the prognosis value of IGs in COAD and conduct a prognosis model for clinical utility. Gene expression data of COAD were downloaded from The Cancer Genome Atlas (TCGA), screening and analyzing differentially expressed IGs by bioinformatics. Core genes were screened by univariate and multivariate Cox regression analyses. Survival analysis was appraised by the Kaplan–Meier method and the log-rank test. Gene Ontology, Kyoto Encyclopedia of Genes and Genomes, and Gene Set Enrichment Analysis (GSEA) were used to identify IGs' relevant signal pathways. We predicted the overall survival (OS) by nomogram. Finally, a prognosis model was conducted based on 12 IGs (*SLC10A2*, *CXCL3*, *NOX4*, *FABP4*, *ADIPOQ*, *IGKV1-33*, *IGLV6-57*, *INHBA*, *UCN*, *VIP*, *NGFR*, and *TRDC*). The risk score was an independent prognostic factor, and a nomogram could accurately predict the OS of individual COAD patients. These results were validated in GSE39582, GSE12945, and GSE103479 cohorts. Functional enrichment analysis demonstrated that these IGs are mainly enriched in hormone secretion, hormone transport, lipid transport, cytokine–cytokine receptor interaction, and peroxisome proliferators-activated receptor signaling pathway. In summary, the risk score is an independent prognostic biomarker. We also excavated several IGs related to COAD's survival and maybe potential biomarkers for COAD diagnosis and treatment.

Introduction

Colorectal cancer is the fourth of the new cases and deaths among 36 cancers in 2018 [1]. It is also the second most frequent cancer diagnosed in women and the third most in men [2]. Several clinical trials have shown that the enhancement of tumor immune response can lead to long-term clinical response and benefit. Many expression profiling studies have proved that there is a relationship between the immune genes' (IGs) characteristics and the better prognosis or efficacy to therapy, either chemotherapy or immunotherapy in tumors [3,4]. It is also essential to understand the immune environment's contribution and the molecular subtypes of different tumor indications, but it lacks adequate wisdom to promote a reasonable combination of immunotherapy [5,6].

Whole genome-wide gene expression clusters such as The Cancer Genome Atlas (TCGA) have been constructed to classify and identify genomic abnormalities in large populations worldwide to detect the effects of the genetic composition of tumors on clinical prognosis [7]. With the human genome map finished, gene expression profiling has been cumulatively accepted by clinical diagnostic criteria. Besides, tumor microenvironment (TME) has significantly influenced therapeutic response and clinical outcomes [8,9]. Transcription and genomic data stemmed from many tumor samples used to research the TME, and immune infiltration assessment illustrated molecular subtypes of acute myeloid leukemia, bladder cancer,

*These authors contributed equally to this work.

Received: 23 May 2020
Revised: 15 October 2020
Accepted: 02 November 2020

Accepted Manuscript online:
03 November 2020
Version of Record published:
17 November 2020

and cervical cancer [10–12]. Several separate reports about immune infiltration and lncRNA were associated with colon adenocarcinoma (COAD) [13,14]. Immunoscore, the primary significant prognostic ability, and robustness in COAD were validated [15]. However, few studies on the combination of IG and immune infiltration in the prognosis model of COAD patients.

The present paper mainly attempted to construct the prognosis model based on prognosis-related IGs (PRIGs), explore the prognostic value, and inquiry immune infiltration in COAD, which provide a novel orientation to the potential targets. Besides, we validated the PRIGs signature in GSE39582, GSE12945, and GSE103479 cohorts. In summary, we identified a new essential marker (risk score) to predict COAD patients' prognosis. Comparison with the previous research, our study provided a new risk model as an independent prognostic biomarker in risk stratification for COAD patients.

Materials and methods

Data sources

In the present study, both the transcriptome and clinical data of COAD were obtained from the TCGA database (Data Release 20.0, Release Date: 11 November 2019, <https://tcga-data.nci.nih.gov/tcga/>). The main filter criteria for our data were as follows: (1) The keywords for cases were colon [Primary Site], 'TCGA [Program]', 'TCGA-COAD [Project]', 'Adenomas and Adenocarcinomas [Disease Type]'. (2) The keywords for files for RNA-sequencing data were 'Transcriptome Profiling [Data Category]', 'Gene Expression Quantification [Data Category]', 'RNA-Seq [Experimental Strategy]', 'HTSeq - FPKM [Workflow Type]'. (3) The keywords for files for clinical data were 'Clinical [Data Category]', 'BCR XML [Data Format]'. The expression of mRNA was obtained from the RNA-sequencing data. The data access (GSE39582, GSE12945, and GSE103479), as the validation data, was obtained from Gene Expression Omnibus (GEO, <https://www.ncbi.nlm.nih.gov/geo/>) database. Gene chips' raw data were normalized using the Robust Multi-Array Average (RMA) algorithm provided by 'limma' [16]. Perl and R-package 'sva' were used to merge microarray data and reduce heterogeneity among the GSE39582, GSE12945, and GSE103479 datasets [17]. We use R software (version 3.6.2) to extract and annotate the expression of immune genes in TCGA and GEO databases.

Bioinformatics analysis of the data

Identification of differential expression of genes, IGs, and transcription factors

Data extraction and integration were performed by Perl software. Screening differentially expressed genes, IGs, transcription factors (TFs) was undertaken by the Wilcoxon Test [16], using R-package 'limma' 'edgeR'. False-discovery rate (FDR) < 0.05 and $\log_2 | \text{fold change, FC} | > 1.5$ were set as the cutoffs. Bidirectional hierarchical clustering was analyzed and heat map was drawn by R-package 'pheatmap' (<https://cran.r-project.org/web/packages/pheatmap/>). R-package 'ggplot2' was used to draw a volcano map. Correlation analysis between differentially expressed IGs (DEIGs) and TFs (DETFs) was performed using correlation tests based on R software ($\text{cor} > 0.4$, $P < 0.001$). The protein–protein interaction (PPI) network was constructed by Cytoscape software (version 3.7.2) [18]. R-package 'Survival' was used to conduct univariate cox regression analysis ($P < 0.01$). Forest map was drawn by the R language 'ggforest' function.

Building a prognosis model of IGs and survival analysis

We constructed an optimal prognosis model of PRIGs via the Akaike Information Criterion. Genes expression and survival analysis were evaluated by the Kaplan–Meier method and the log-rank test ($P < 0.05$). The risk score of each patient was calculated by the following formula: Risk score = $\sum_{j=1}^n \text{Coef}_j \times X_j$, where, Coef_j denotes the coefficient and X_j indicates the expression levels of each IG [19]. The survival data were obtained from the clinical data and combined with the previously acquired expression profiling data. The median risk score was selected as a cutoff to divide COAD cohorts into high-risk and low-risk groups. The evaluation indicator of survival analysis was overall survival (OS), which refers to the period from the date of diagnosis until death from any cause. The survival curve was drawn according to the high- and low-risk value using R-package 'survival' and 'survminer.' R-package 'survival ROC' was used to draw the Receiver Operating Characteristic (ROC) curve for the difference and calculate the value of Area Under Curve (AUC). The risk curve, survival state diagram, and heat map were drawn based on the patient risk score. PRIGs were recognized by univariate and multivariate Cox regression analyses. The results were verified in the GSE39582, GSE12945, and GSE103479 cohorts.

The exploitation of the nomogram

We used the expression of PRIGs to draw a nomogram via the R-package ‘Hmisc,’ ‘lattice,’ ‘Formula,’ ‘ggplot2,’ ‘foreign,’ and ‘rms.’ Moreover, calibration curves were used to assess the consistency between actual and predicted survival rates. Furthermore, the consistency index (C-index) was calculated to evaluate the model prognosis capability. The values of 0.5 and 1.0 represent a random probability and an excellent performance for predicting survival with the model, respectively. The GSE39582, GSE12945, and GSE103479 cohorts were used to verify the risk score’s prognostic value and the nomogram.

Functional enrichment analysis of PRIGs and immune cells infiltration in COAD

Based on the R software, the functional enrichment analysis of PRIGs was performed to identify Gene Ontology (GO) categories of biological processes (BPs) and molecular functions (MFs). The Database for Annotation, Visualization and Integrated Discovery (DAVID) database was used to conduct enrichment analysis of Kyoto Encyclopedia of Genes and Genomes (KEGG) pathways [20]. FDR < 0.05 was invoked as the cutoff. R-package ‘GOplot’ was used to integrate expression data and functional enrichment analysis. Moreover, Gene Set Enrichment Analysis (GSEA) was also used to analyze the differences between the high-risk and low-risk groups. The number of permutations was set to 1000 and FDR < 0.25 was acknowledged as statistically significant [21].

Results

Characteristics of patients

TCGA-COAD cohort included 385 patients. Patients without survival time and less than 90 days were excluded, and 334 patients were obtained as the training group. GSE39582 dataset included 566 stage I–IV COAD patients, GSE12945 contained 62 stages I–IV colorectal cancer patients, and GSE103479 included 156 stage I–IV colorectal cancer patients. Using the same exclusion criteria of the training group, 587 colorectal cancer patients were selected from the GEO cohorts as the test group. The detailed clinical characteristics of patients are listed in Supplementary Table S1.

Identification of differentially expressed genes, IGs, and TFs

A total of 437 transcriptome data were obtained, 39 (8.9%) were derived from healthy samples and 398 cases (91.1%) came from tumor samples. We screened out 3833 differentially expressed genes (DEGs) included 2610 up-regulated and 1223 down-regulated (Figure 1A,D); 332 differentially expressed immune genes (DEIGs) contained 120 up-regulated and 212 down-regulated (Figure 1B,E). We also obtained 37 differentially expressed transcription factors (DETFs) including 25 up-regulated and 12 down-regulated (Figure 1C,F).

Prognosis model of immune constructed and survival analysis

We filtered out 24 PRIGs by univariate Cox regression analysis. CXCL3 was low-risk PRIG (Hazard Ratio (HR) < 1, $P < 0.01$), others were high-risk PRIGs (HR > 1, $P < 0.01$); the detailed information is shown in Supplementary Figure S1 and Table S2. Twelve PRIGs were selected by multivariate regression analysis, including *SLC10A2*, *CXCL3*, *NOX4*, *FABP4*, *ADIPOQ*, *IGKV1-33*, *IGLV6-57*, *INHBA*, *UCN*, *VIP*, *NGFR*, and *TRDC* (Table 1). The prognosis model was constructed based on these 12 PRIGs. The coefficient of PRIGs is shown in Supplementary Figure S2. Each patient’s risk score was computed based on each gene’s expression level and risk coefficient. A risk score was used to predict prognosis.

The calculation formula of the risk score was as follows: Risk score = $0.1966 \times$ expression of TRDC + $(-0.3930) \times$ expression of NGFR + $0.0473 \times$ expression of VIP + $0.4528 \times$ expression of UCN + $0.1227 \times$ expression of INHBA + $0.0027 \times$ expression of IGLV6-57 + $0.0625 \times$ expression of IGKV1-33 + $(-0.3076) \times$ expression of ADIPOQ + $0.0692 \times$ expression of FABP4 + $(-1.1528) \times$ expression of NOX4 + $(-0.0249) \times$ expression of CXCL3 + $0.6105 \times$ expression of SLC10A2.

According to the median risk score, the patients were divided into high-risk and low-risk groups. A heat map visualized the gene expression profiles of the high- and low-risk groups. As the risk score escalated, the patients’ survival time decreased, and the death numbers increased (Figure 2A). In the training group, the Venn diagram and R software were used to select the validation gene by intersecting with the 24 prognostic-related IGs screened from the TCGA database, and finally 5 genes were verified (Figure 2B). OS was significantly lower in the high-risk subgroup than in the low-risk subgroup (Figure 2C, $P = 1.294e-05$), the 1-, 3-, and 5-year AUC value of ROC was 0.792, 0.744, and 0.797, respectively (Figure 2D). Similarly, in the test group, OS was also apparently lower in the high-risk subgroup than in the low-risk subgroup (Figure 2E, $P = 2.178e-05$), and the 1-, 3-, and 5-year AUC value

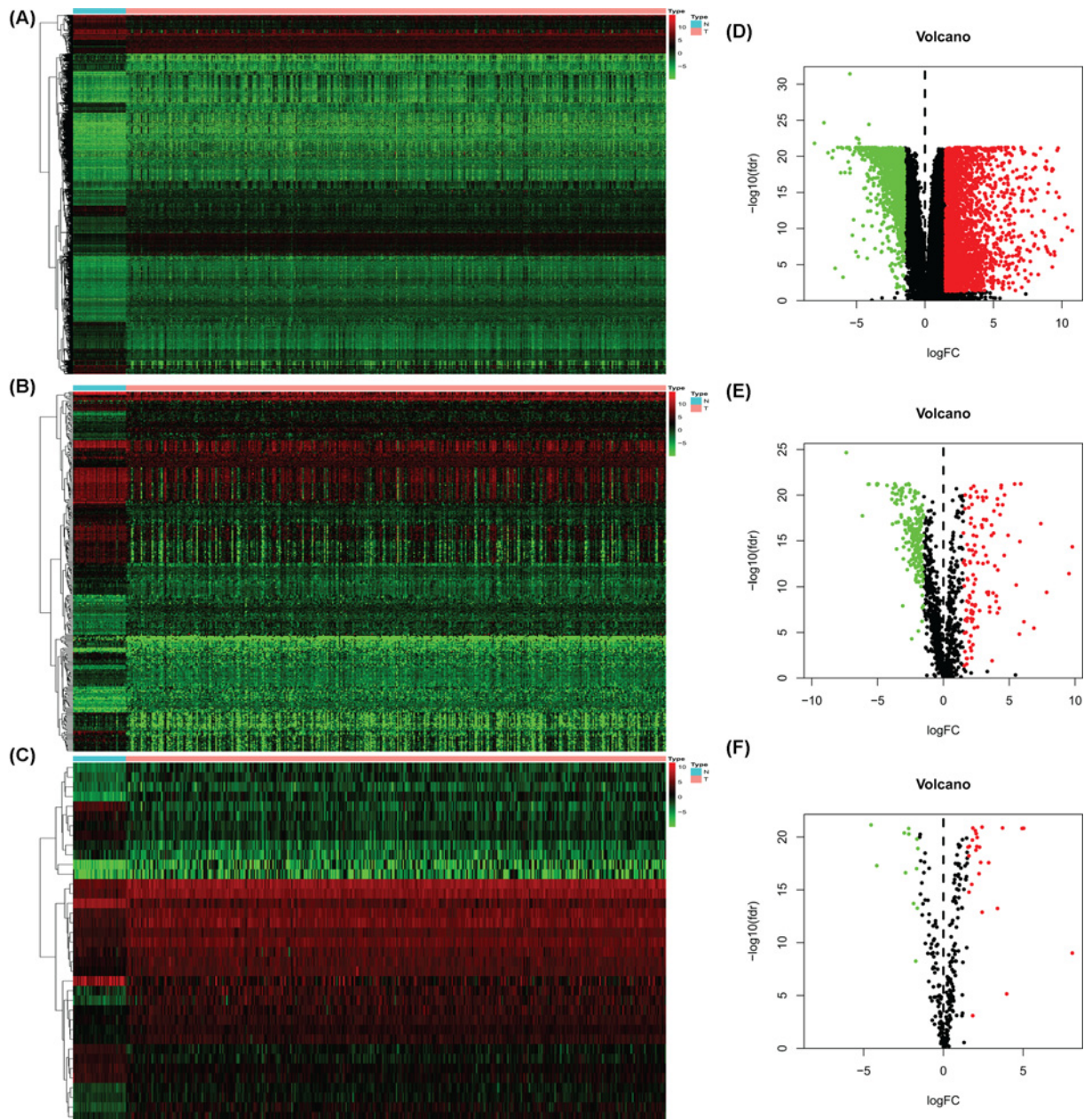


Figure 1. Differentially expressed genes, IGs, and TFs in TCGA-COAD

Heatmaps: DEGs (A), DEIGs (B), and DETFs (C); higher expression manifested in red; lower expressions were green. Volcano diagrams: DEGs (D), DEIGs (E), and DETFs (F); each point represents a gene. Down-regulated (green), up-regulated (red), and no significance DEGs, DIEGs, DTFs (black). IGs, immune genes; TFs, transcription factors; TCGA, The Cancer Genome Atlas; COAD, colon adenocarcinoma; DEGs, differentially expressed genes; DEIGs, differentially expressed immune genes; DETFs, differentially expressed transcription factors.

of ROC was 0.625, 0.646, and 0.713, respectively (Figure 2F). Univariate and multivariate independent prognostic analyses manifested that the risk score was an independent prognostic predictor both in the training and test groups (Tables 2 and 3, Supplementary Figure S3).

A characterized prognostic prediction model

Nomogram is a useful tool quantifying an individual's risk in a clinical setting by integrating multiple risk factors [22,23]. We exploited the nomogram to predict 3- and 5-years OS probabilities by integrating the 12 PRIGs signature

Table 1 PRIGs (multivariate Cox regression analysis) and prognosis model coefficient

PRIGs	Coefficient	HR	95% CI	P-value
SLC10A2	0.6105	1.8413	1.1402–2.9734	0.0125
CXCL3	−0.0249	0.9754	0.9567–0.9945	0.0119
NOX4	−1.1528	0.3157	0.0985–1.0122	0.0524
FABP4	0.0693	1.0717	1.0286–1.1167	0.0009
ADIPOQ	−0.3076	0.7352	0.5597–0.9657	0.0270
IGKV1-33	0.0626	1.0646	1.0186–1.1126	0.0054
IGLV6-57	0.0027	1.0027	1.0012–1.0042	0.0004
INHBA	0.1227	1.1306	1.0327–1.2377	0.0079
UCN	0.4528	1.5727	1.2582–1.9658	0.0001
VIP	0.0473	1.0485	0.9867–1.1141	0.1266
NGFR	−0.3930	0.6750	0.4345–1.0489	0.0805
TRDC	0.1966	1.2173	1.0900–1.3595	0.0005

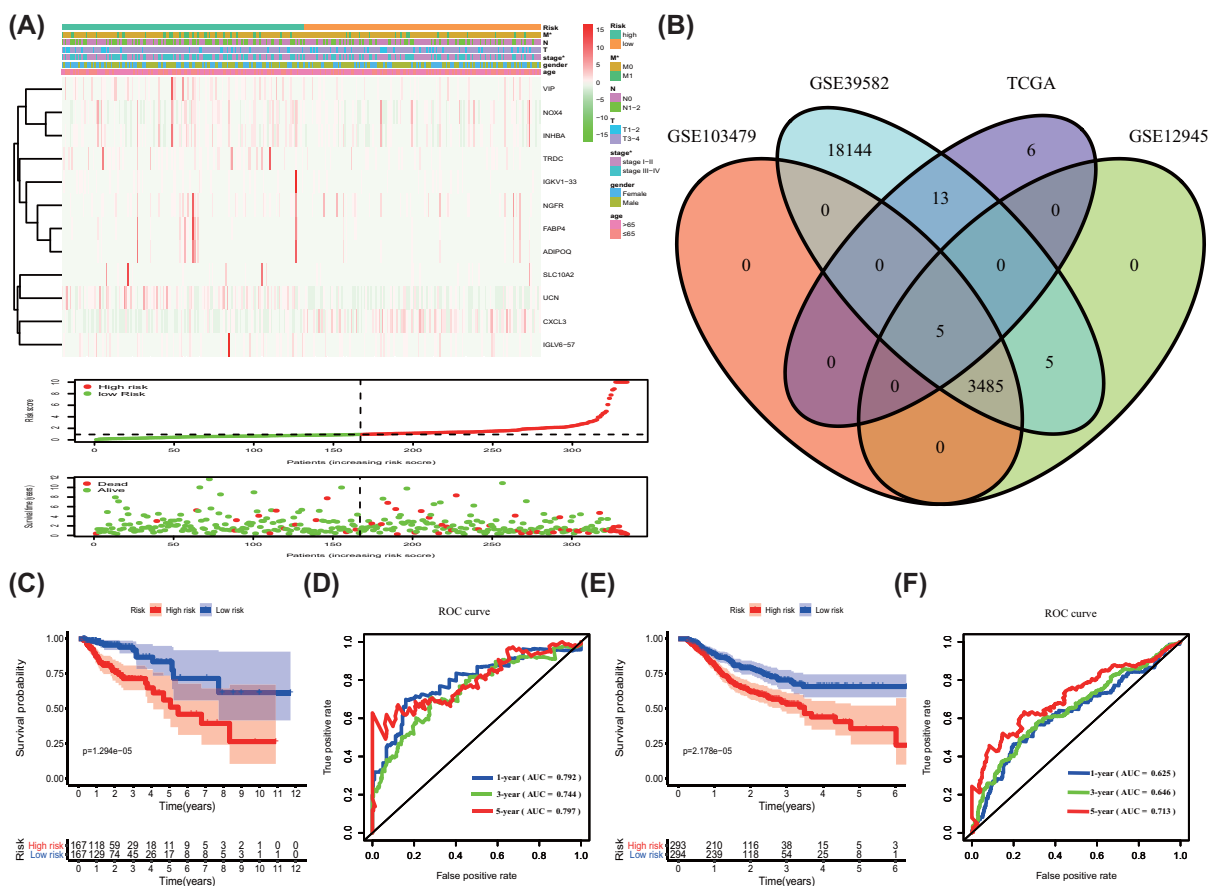


Figure 2. Prognosis model of IGs and survival analysis

(A) Heatmap of the immune-associated gene expression profiles in prognostic signature for TCGA-COAD. The distribution of risk score and patient's survival time, as well as the survival status of TCGA-COAD. The black dotted line is the optimum cutoff dividing patients into low- and high-risk groups. * represented $P < 0.05$. (B–F) Kaplan–Meier survival analysis of COAD patients ranked by the median risk score. The high-risk score was related to poor OS in training group (C) and test group (E). ROC analysis of the sensitivity and specificity of the OS in training group (D) and test group (F). OS, overall survival; ROC, Receiver Operating Characteristic.

Table 2 The prognostic value of different clinical characteristics in the training group

Variables	Univariate prognostic analysis			Multivariate prognostic analysis		
	HR	95% CI	P-value	HR	95% CI	P-value
Age (≤ 65 vs. > 65 years)	1.7361	0.8958–3.3647	0.1023	2.4514	1.1910–5.0456	0.0149
Gender (female vs. male)	1.1784	0.6496–2.1375	0.5890	0.9428	0.5054–1.7587	0.8530
Stage (I/II vs. III/IV)	4.5987	2.3719–8.9160	6.28E-06	2.1689	0.2393–19.6625	0.4912
T (1–2 vs. 3–4)	9.5372	1.3085–69.5115	0.0261	3.8526	0.5048–29.4052	0.1933
N (0 vs. 1–3)	4.2744	2.2413–8.1519	1.03E-05	1.2869	0.1687–9.8185	0.8078
M (0 vs. 1)	6.6080	3.6126–12.0868	8.84E-10	3.4409	1.6652–7.1102	0.0008
Risk score	1.0069	1.0037–1.0101	2.46E-05	1.0051	1.0018–1.0083	0.0021

Table 3 The prognostic value of different clinical characteristics in the test group

Variables	Univariate prognostic analysis			Multivariate prognostic analysis		
	HR	95% CI	P-value	HR	95% CI	P-value
Age (≤ 65 vs. > 65 years)	1.3467	0.9954–1.8221	0.0536	1.4041	1.0328–1.9087	0.0303
Gender (female vs. male)	1.2162	0.9046–1.6352	0.1950	1.2656	0.9367–1.7101	0.1250
Stage (I/II vs. III/IV)	2.0615	1.5306–2.7766	1.92E-06	2.2131	1.6259–3.0124	4.42E-07
T (1–2 vs. 3–4)	2.0090	1.0613–3.8027	0.0321	1.3989	0.7332–2.6689	0.3084
N (0 vs. 1–3)	0.9644	0.7186–1.2943	0.8091	0.7357	0.5394–1.0034	0.0526
M (0 vs. 1)	1.2951	0.8288–2.0235	0.2562	1.4461	0.9076–2.3042	0.1207
Risk score	1.7018	1.4854–1.9498	1.84E-14	1.6438	1.4254–1.8958	8.44E-12

for TCGA-COAD and verified in the GEO datasets (Figure 3A). Each factor is assigned a score in proportion to its contribution to the survival risk. We calculated each patient's total points by summarizing the number of points for all PRIGs and estimating survival rates via drafting a vertical line between each prognosis axis and the total point axis, which may help appropriate practitioners make clinical decisions for COAD patients. The calibration curve showed that the actual survival rate matched the predicted 3- and 5-years survival rate well; the C-index was 0.77 in the TCGA data (Figure 3B–D). The nomogram was verified in the GEO cohorts, the C-index was 0.72, and 3- and 5-year calibration curves were shown in Figure 3E–G.

Functional enrichment analysis of PRIGs and immune cells infiltration in TCGA-COAD

The PPI networks between DIGs and DTFs were made up of ten DEIGs and four DETFs. All of them had a positive relationship (correlation coefficient = 0.4, $P < 0.001$, Figure 4A). GO enrichment analysis of the 12 PRIGs manifested in Figure 4B,C, a total of 36 GO terms of BP, 26 GO terms of MF were identified to be significant (Supplementary Material S1, $FDR < 0.05$). These 12 genes were involved in several essential BPs, including hormone secretion, hormone transport, lipid transport, lipid localization, signal release, macrophage differentiation regulation, negative regulation of blood pressure, and negative regulation of secretion, glucose homeostasis, brown fat cell differentiation. The TOP-10 terms of BP and MF are shown in Figure 4C.

The KEGG pathway analysis showed that PRIGs are mainly enriched in the cytokine–cytokine receptor interaction, Peroxisome Proliferators-activated Receptor (PPAR) signaling pathway ($P < 0.05$). GSEA analysis showed that changed genes were enriched in several common pathways. A total of 111/178 genesets were up-regulated in phenotype high-risk group, 66 gene sets were significant at $FDR < 25\%$. The top-eight of the high-risk group are shown in Figure 4D, including hedgehog signaling pathway (Enrichment score, $NES = 2.09$, $P = 0.000$), basal cell carcinoma ($NES = 1.98$, $P = 0.000$), axon guidance ($NES = 1.87$, $P = 0.004$), notch signaling pathway ($NES = 1.86$, $P = 0.010$), Gonadotropin-releasing hormone (GnRH) signaling pathway ($NES = 1.84$, $P = 0.002$), glycosaminoglycan biosynthesis chondroitin sulfate ($NES = 1.83$, $P = 0.006$), extracellular matrix (ECM) receptor interaction ($NES = 1.77$, $P = 0.025$), and dorsoventral axis formation ($NES = 1.77$, $P = 0.011$).

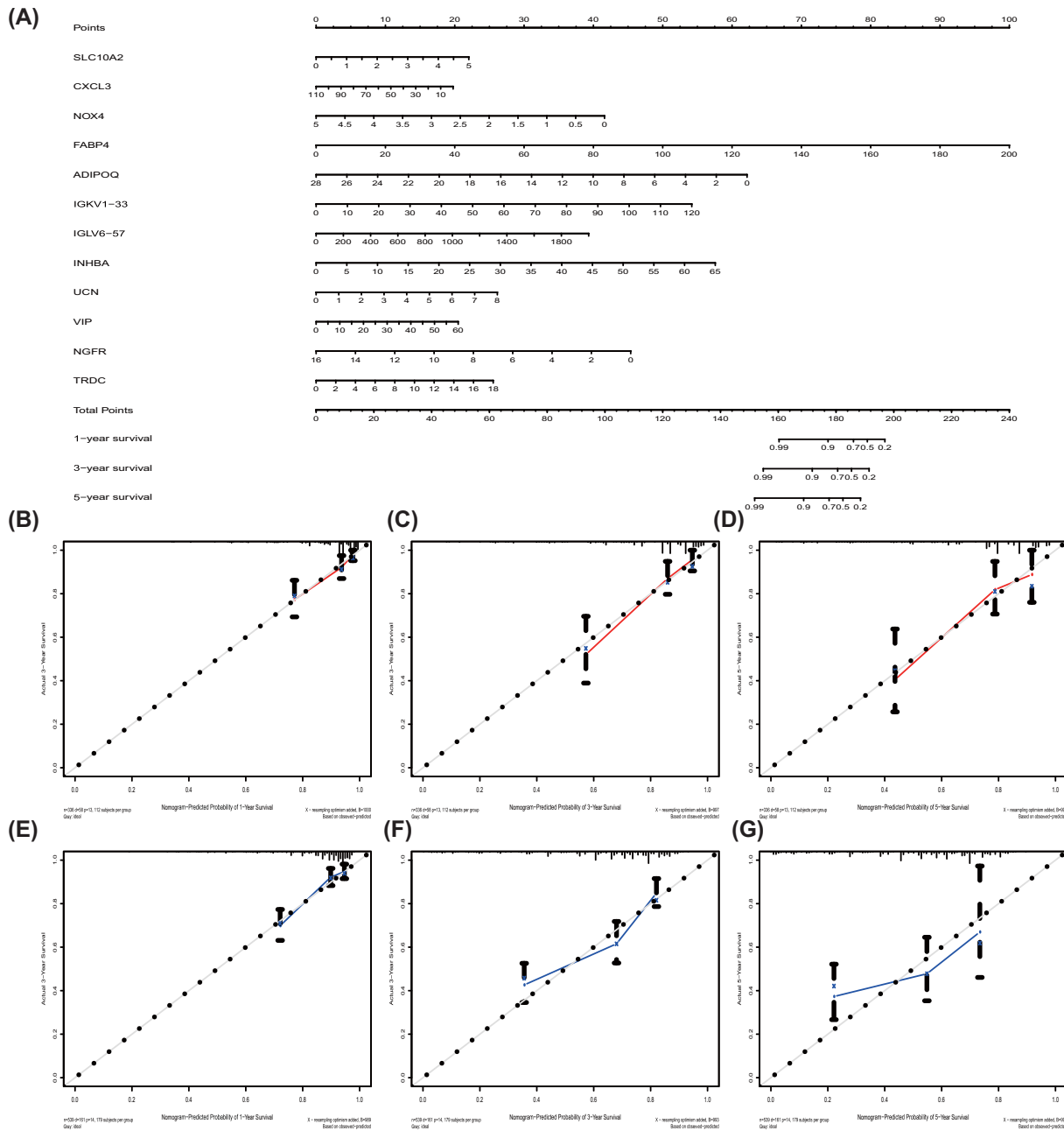


Figure 3. The nomogram to anticipate prognostic probabilities in COAD

(A) The nomogram for predicting 1-, 3-, and 5-year OS of TCGA-COAD by 12 PRIGs signature. (B–G) The nomogram for predicting 1-, 3-, and 5-year OS of COAD by gene expression. (B–D) TCGA dataset and (E–G) GEO dataset. OS, overall survival.

Discussion

The diagnostic strategy for evaluating the tumor immune infiltration has a comprehensive clinical application value. Although the overlapping biological features of tumor immunophenotypes have been described [3], gene composition lacks consensus, the cell specificity of gene expression signal is not apparent, and there is no systematic analysis of the gene's prognostic value in various tumor types. Until recently, a comprehensive meta-analysis confirmed the prognostic role of the IG in cancer as a whole [24]. In the current work, we singled out 24 PRIGs and constructed a

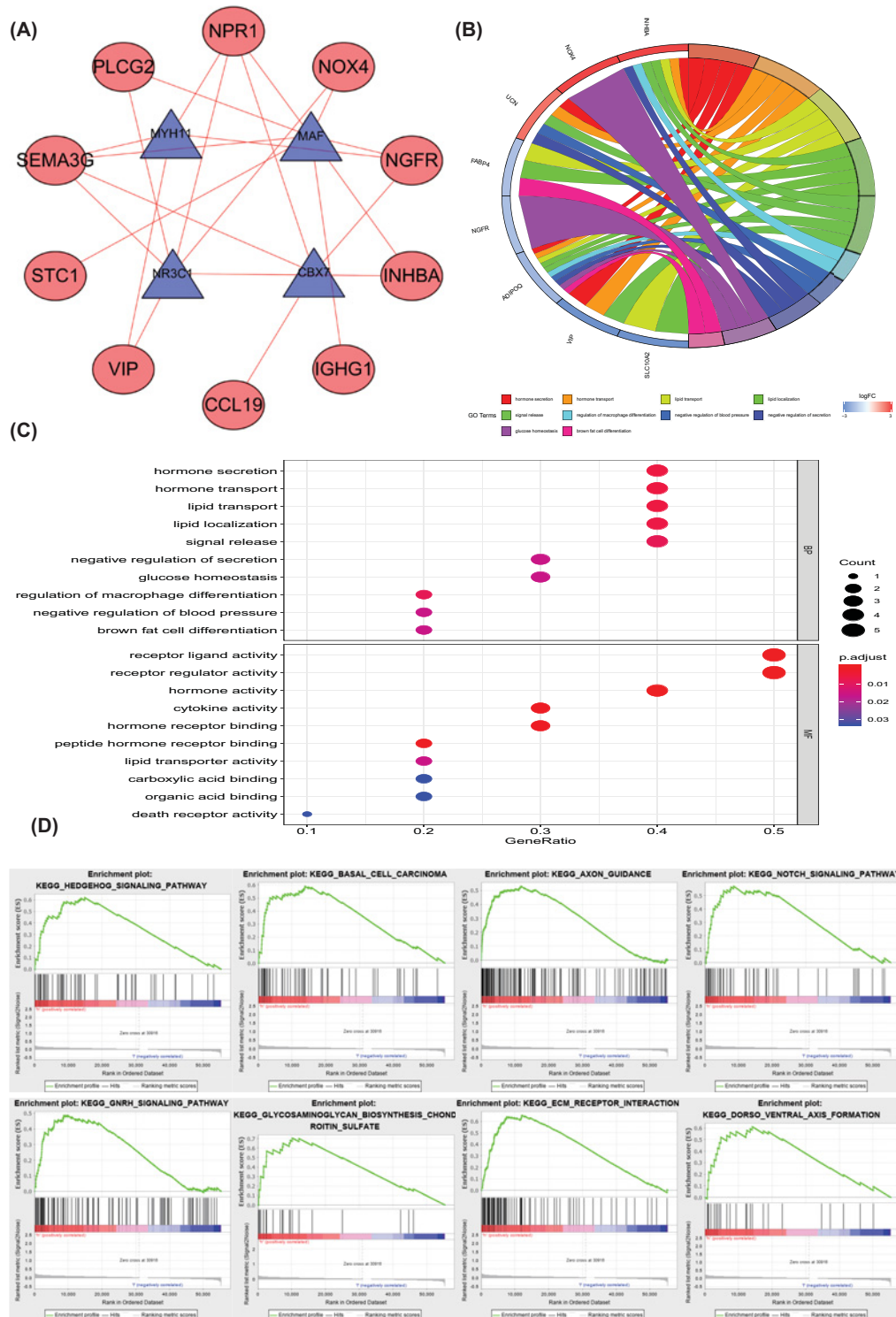


Figure 4. PPI networks and functional enrichment analysis of PRIGs

(A) PPI networks: the positive interactions (red line), TFs (blue and triangle), high-risk IGs (red and ellipse). **(B)** GO terms of PRIGs: on the left is the gene, up-regulation was red and down-regulation was blue, on the right was a different GO term, and the genes were linked via ribbons to their assigned terms ($P < 0.05$). **(C)** The TOP-10 terms of BP and MF. **(D)** GSEA analysis of the differentially expressed genes in the high-risk group. PRIGs, prognosis-related immune genes; PPI, Protein-Protein interaction; GO, Gene Ontology; BP, biological processes; MF, molecular functions; GSEA, Gene Set Enrichment Analysis.

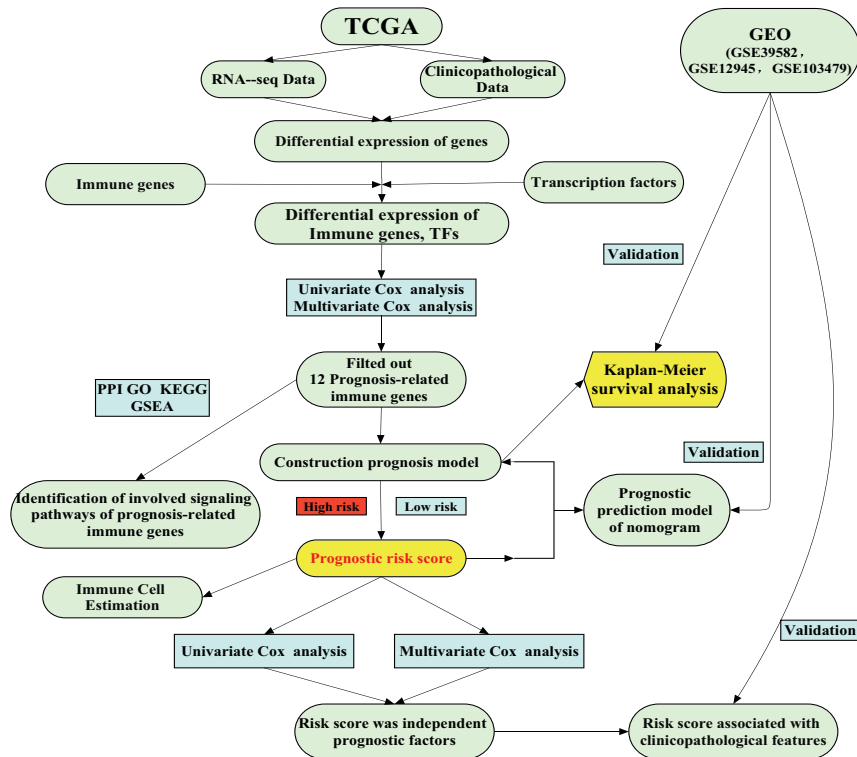


Figure 5. A flowchart of the study design and analysis

prognosis model based on 12 PRIGs, which was entirely accurate and had better predictive value. A short bioinformatics protocol flow chart listed in Figure 5.

First, univariate regression analysis demonstrated that 22 genes had a relationship with poor prognosis, especially *SLC10A2*, *PLCG2*, and *PTH1R*. Previous reports have mentioned that secondary bile acids increase the risk of COAD, and *SLC10A2* plays a crucial role in intestinal bile acid reabsorption. This transporter is the primary mechanism for the uptake of intestinal bile acids by apical cells in the distal ileum. Bile acid malabsorption is related to epidermal growth factor receptor expression and M3 muscarinic [25,26]. *PLCG2* is associated with immune responses and *PLCG2* mutations have been found in the chronic lymphocytic leukemia patient [27,28]. However, its role in COAD's occurrence and development is not very clear, and is worth further study. Researchers found that *PTH1R* was associated with both miRNA and DNA methylation in colorectal liver metastasis patients [29].

Second, whether the IG expression can be used as a prognostic marker is a vital research topic. In the present study, our prognosis model is considered to be valuable. The 1-, 3-, and 5-year AUC values of ROC were 0.792, 0.744, and 0.797, respectively, which was more accurate than previous reports [30,31]. The 12 IGs may be ideal prognostic markers. Five-year OS was ~75% in the low-risk group and 50% in the high-risk group, consistent with the previous report [32]. High-risk genes in the model, including *SLC10A2*, *NOX4*, *FABP4*, *ADIPOQ*, *IGKV1-33*, *IGLV6-57*, *INHBA*, *UCN*, *VIP*, *NGFR*, and *TRDC*. NADPH oxidase complex can positively predict relapse in stage II left-side COAD, *NOX4* encodes a member of the NOX-family of enzymes that functions as the catalytic subunit [33]. *FABP4* plays a crucial role in regulating lipid metabolism and adipocyte differentiation associated with the tumor suppressor, *PTEN* [34]. *FABP4* and *ADIPOQ* have been reported to increase the risk of colorectal neoplasia related to the COAD survival probability [35,36]. Dudgeon et al. found that *UCN* can inhibit COAD cell growth via inducing apoptosis by *PUMA* and a *p53* target [37]. *VIP* promotes the initiation and progression of COAD by the generation of a local proinflammatory environment [38]. *NGFR* hypermethylation can be observed through COAD development [39]. The risk score is closely correlated with the COAD malignant clinicopathological characteristics and is an independent prognostic factor. The prediction ability of 12 immune genes is also cross-verified in three GEO data sets, which shows that our cohort analysis based on TCGA and GEO data has predictive value. Moreover, the roles of *IGKV1-33*, *IGLV6-57*, and *TRDC* in the development of COAD are not very clear, which deserve further study.

Subsequently, we constructed a nomogram to predict individual clinical outcomes. Nomogram is a stable and reliable tool to quantify individual risk by combining and describing risk factors, which has been used for tumor prognosis, including colorectal cancer [40,41]. By summarizing all points of view, the model provides individuals with numerical possibilities for clinical outcomes, such as OS, relapse, and drug noncompliance. Except for standard clinicopathological features, such as genetic markers, can also be included in predictive nomogram models to predict clinical outcomes [41,42]. The combination of autophagy gene features and prognostic factors has a better prognostic value than a single application [43]. Besides, the calibration curve showed that the nomogram accurately predicted 3- and 5-years survival rates. Consistently, in the current study, we illustrated that a nomogram, including the 12 PRIGs signature, could better predict the 3- and 5-years survival possibility of COAD patients. These results suggest that the 12-PRIGs prognostic model maybe have a convinced value in adjusting COAD patients' treatment plans.

Furthermore, GO enrichment and KEGG pathway analysis show that PRIG participates in regulating several crucial processes and signaling pathways. ADIPOQ, INHBA, UCN, and VIP participate in hormone secretion and hormone transport BPs. SLC10A2, FABP4, ADIPOQ, and INHBA involved in lipid transport and lipid localization BPs [44–46]; INHBA, CXCL3, and NGFR participate in the regulation of the cytokine–cytokine receptor interaction pathway; FABP4 and ADIPOQ involved in the regulation of PPAR signaling pathway, which coincided with the previous report, PPAR signaling pathway might affect the recurrence of COAD patients [47,48]. The GSEA analysis further suggested that the pro-tumor inflammatory reaction might be more prominent in stage IIB/IIC of COAD [49]. The blockade of PD-L1 increased FABP4 expression in tissue-resident memory T (Trm) cells, promoting lipid uptake by Trm cells [50]. Previous reports indicate that the hedgehog signaling pathway might affect the recurrence of COAD patients [51]. Dandawate et al. reported that the Notch signaling pathway involved regulating colon cancer cells' proliferation [51]. Our results are consistent with these reports.

From the above discussion, the conclusion can be reached that 12 IGs were more significantly associated with the COAD prognosis and the prognosis model was accurate. The prognostic model based on these genes is validated in three independent GEO cohorts. Further research might be necessary about these genes in the clinical application and may provide a new perspective into the COAD's pathogenesis. Some of the antecedently overlooked genes maybe have a chance to become additional biomarkers for COAD. Finally, the present study enhanced our cognition of the sophistication of the occurrence and development of COAD and may detect novel therapeutic targets.

Data Availability

The authors certify that all the original data in this research could be obtained from public database. Both the transcriptome and clinical data of COAD were obtained from the TCGA database (<https://tcga-data.nci.nih.gov/tcga/>). The data of training group are available at NCBI GEO (GSE39582 <https://www.ncbi.nlm.nih.gov/geo/query/acc.cgi?acc=GSE39582>, GSE12945 <https://www.ncbi.nlm.nih.gov/geo/query/acc.cgi?acc=GSE12945>, and GSE103479 <https://www.ncbi.nlm.nih.gov/geo/query/acc.cgi?acc=GSE103479>). Other data that were used to support the findings of the present study are included within the supplementary information files. All the raw data in the present study are available from the first author or corresponding author upon request.

Competing Interests

The authors declare that there are no competing interests associated with the manuscript.

Funding

The authors declare that there are no sources of funding to be acknowledged.

Author Contribution

D.h.M. and Y.d.M. designed the study. X.p.M. downloaded the data. Y.d.M. and Y.Y. analyzed the data. Y.d.M. and J.t.W. drafted the article. All authors approved the paper.

Acknowledgements

We thank the TCGA and GEO databases for the availability of the data.

Abbreviations

AUC, Area Under Curve; BP, Biological Process; COAD, Colon Adenocarcinoma; C-index, Consistency Index; DAVID, The Database for Annotation, Visualization and Integrated Discovery; DEG, Differentially Expressed Gene; DEIG, Differentially Expressed Immune Gene; DETF, Differentially Expressed Transcription Factor; ECM, Extracellular Matrix; GEO, Gene Expression

Omnibus; GnRH, Gonadotropin-releasing Hormone; GO, Gene Ontology; GSEA, Gene Set Enrichment Analysis; HR, Hazard Ratio; IG, Immune Gene; KEGG, Kyoto Encyclopedia of Genes and Genomes; MF, Molecular Function; NES, Enrichment Score; OS, Overall Survival; PPAR, Peroxisome Proliferators-activated Receptor; PPI, Protein-Protein Interaction; PRIG, Prognosis-related IGs; RMA, Robust Multi-Array Average; ROC, Receiver Operating Characteristic; TCGA, The Cancer Genome Atlas; TF, Transcription Factor; TME, Tumor Microenvironment; TrmR, Resident memory T cell.

References

- 1 Bray, F., Ferlay, J., Soerjomataram, I., Siegel, R.L., Torre, L.A. and Jemal, A. (2018) Global cancer statistics 2018: GLOBOCAN estimates of incidence and mortality worldwide for 36 cancers in 185 countries. *CA Cancer J. Clin.* **68**, 394–424, <https://doi.org/10.3322/caac.21492>
- 2 Dekker, E., Tanis, P.J., Vleugels, J.L.A., Kasi, P.M. and Wallace, M.B. (2019) Colorectal cancer. *Lancet* **394**, 1467–1480, [https://doi.org/10.1016/S0140-6736\(19\)32319-0](https://doi.org/10.1016/S0140-6736(19)32319-0)
- 3 Galon, J., Angell, H.K., Bedognetti, D. and Marincola, F.M. (2013) The continuum of cancer immunosurveillance: prognostic, predictive, and mechanistic signatures. *Immunity* **39**, 11–26, <https://doi.org/10.1016/j.immuni.2013.07.008>
- 4 Bedognetti, D., Hendrickx, W., Marincola, F.M. and Miller, L.D. (2015) Prognostic and predictive immune gene signatures in breast cancer. *Curr. Opin. Oncol.* **27**, 433–444, <https://doi.org/10.1097/CCO.0000000000000234>
- 5 Angell, H.K., Bruni, D., Barrett, J.C., Herbst, R. and Galon, J. (2020) The immunoscore: colon cancer and beyond. *Clin. Cancer Res.* **26**, 332–339, <https://doi.org/10.1158/1078-0432.CCR-18-1851>
- 6 Pagès, F., Mlecnik, B., Marliot, F., Bindea, G., Ou, F.S., Bifulco, C. et al. (2018) International validation of the consensus Immunoscore for the classification of colon cancer: a prognostic and accuracy study. *Lancet* **391**, 2128–2139, [https://doi.org/10.1016/S0140-6736\(18\)30789-X](https://doi.org/10.1016/S0140-6736(18)30789-X)
- 7 Cancer Genome Atlas Research Network (2008) Comprehensive genomic characterization defines human glioblastoma genes and core pathways. *Nature* **455**, 1061–1068, <https://doi.org/10.1038/nature07385>
- 8 Wu, T. and Dai, Y. (2017) Tumor microenvironment and therapeutic response. *Cancer Lett.* **387**, 61–68, <https://doi.org/10.1016/j.canlet.2016.01.043>
- 9 Meurette, O. and Mehlen, P. (2018) Notch signaling in the tumor microenvironment. *Cancer Cell* **34**, 536–548, <https://doi.org/10.1016/j.ccell.2018.07.009>
- 10 Yan, H., Qu, J., Cao, W., Liu, Y., Zheng, G., Zhang, E. et al. (2019) Identification of prognostic genes in the acute myeloid leukemia immune microenvironment based on TCGA data analysis. *Cancer Immunol. Immunother.* **68**, 1971–1978, <https://doi.org/10.1007/s00262-019-02408-7>
- 11 Chen, M., Nie, Z.Y., Wen, X.H., Gao, Y.H., Cao, H. and Zhang, S.F. (2019) m6A RNA methylation regulators can contribute to malignant progression and impact the prognosis of bladder cancer. *Biosci. Rep.* **39**, BSR20192892, <https://doi.org/10.1042/BSR20192892>
- 12 Guo, F., Zhang, B., Chen, C. and Zou, W. (2019) Analysis of CASP12 diagnostic and prognostic value in cervical cancer based on TCGA database. *Biosci. Rep.* **39**, BSR20192706, <https://doi.org/10.1042/BSR20192706>
- 13 Peng, D., Wang, L., Li, H., Cai, C., Tan, Y., Xu, B. et al. (2019) An immune infiltration signature to predict the overall survival of patients with colon cancer. *IUBMB Life* **71**, 1760–1770, <https://doi.org/10.1002/iub.2124>
- 14 Yuan, W., Li, X., Liu, L., Wei, C., Sun, D., Peng, S. et al. (2019) Comprehensive analysis of lncRNA-associated ceRNA network in colorectal cancer. *Biochem. Biophys. Res. Commun.* **508**, 374–379, <https://doi.org/10.1016/j.bbrc.2018.11.151>
- 15 Galon, J., Pages, F., Marincola, F.M., Thurin, M., Trinchieri, G., Fox, B.A. et al. (2012) The immune score as a new possible approach for the classification of cancer. *J. Transl. Med.* **10**, 1, <https://doi.org/10.1186/1479-5876-10-1>
- 16 Ritchie, M.E., Phipson, B., Wu, D., Hu, Y., Law, C.W., Shi, W. et al. (2015) Limma powers differential expression analyses for RNA-seq and microarray studies. *Nucleic Acids Res.* **43**, e47, <https://doi.org/10.1093/nar/gkv007>
- 17 Zhang, S., Wu, Z., Xie, J., Yang, Y., Wang, L. and Qiu, H. (2019) DNA methylation exploration for ARDS: a multi-omics and multi-microarray interrelated analysis. *J. Transl. Med.* **17**, 345, <https://doi.org/10.1186/s12967-019-2090-1>
- 18 Shannon, P., Markiel, A., Ozier, O., Baliga, N.S., Wang, J.T., Ramage, D. et al. (2003) Cytoscape: a software environment for integrated models of biomolecular interaction networks. *Genome Res.* **13**, 2498–2504, <https://doi.org/10.1101/gr.1239303>
- 19 Liu, Y., Wu, L., Ao, H., Zhao, M., Leng, X., Liu, M. et al. (2019) Prognostic implications of autophagy-associated gene signatures in non-small cell lung cancer. *Aging* **11**, 11440–11462, <https://doi.org/10.18632/aging.102544>
- 20 Walter, W., Sanchez-Cabo, F. and Ricote, M. (2015) Gplots: an R package for visually combining expression data with functional analysis. *Bioinformatics* **31**, 2912–2914, <https://doi.org/10.1093/bioinformatics/btv300>
- 21 Miao, Y., Li, Q., Wang, J., Quan, W., Li, C., Yang, Y. et al. (2020) Prognostic implications of metabolism-associated gene signatures in colorectal cancer. *PeerJ* **8**, e9847, <https://doi.org/10.7717/peerj.9847>
- 22 Liang, W., Zhang, L., Jiang, G., Wang, Q., Liu, L., Liu, D. et al. (2015) Development and validation of a nomogram for predicting survival in patients with resected non-small-cell lung cancer. *J. Clin. Oncol.* **33**, 861–869, <https://doi.org/10.1200/JCO.2014.56.6661>
- 23 Won, Y.W., Joo, J., Yun, T., Lee, G.K., Han, J.Y., Kim, H.T. et al. (2015) A nomogram to predict brain metastasis as the first relapse in curatively resected non-small cell lung cancer patients. *Lung Cancer* **88**, 201–207, <https://doi.org/10.1016/j.lungcan.2015.02.006>
- 24 Gentles, A.J., Newman, A.M., Liu, C.L., Bratman, S.V., Feng, W., Kim, D. et al. (2015) The prognostic landscape of genes and infiltrating immune cells across human cancers. *Nat. Med.* **21**, 938–945, <https://doi.org/10.1038/nm.3909>
- 25 Zheng, X., Ekins, S., Raufman, J.P. and Polli, J.E. (2009) Computational models for drug inhibition of the human apical sodium-dependent bile acid transporter. *Mol. Pharm.* **6**, 1591–1603, <https://doi.org/10.1021/mp900163d>
- 26 Raufman, J.P., Dawson, P.A., Rao, A., Drachenberg, C.B., Heath, J., Shang, A.C. et al. (2015) Slc10a2-null mice uncover colon cancer-promoting actions of endogenous fecal bile acids. *Carcinogenesis* **36**, 1193–1200, <https://doi.org/10.1093/carcin/bgv107>

- 27 Qi, F., Qin, W.X. and Zang, Y.S. (2019) Molecular mechanism of triple-negative breast cancer-associated BRCA1 and the identification of signaling pathways. *Oncol. Lett.* **17**, 2905–2914
- 28 Maddocks, K.J., Ruppert, A.S., Lozanski, G., Heerema, N.A., Zhao, W., Abruzzo, L. et al. (2015) Etiology of ibrutinib therapy discontinuation and outcomes in patients with chronic lymphocytic leukemia. *JAMA Oncol.* **1**, 80–87, <https://doi.org/10.1001/jamaoncol.2014.218>
- 29 Liu, J., Li, H., Sun, L., Shen, S., Zhou, Q., Yuan, Y. et al. (2019) Epigenetic alternations of microRNAs and DNA methylation contribute to liver metastasis of colorectal cancer. *Dig. Dis. Sci.* **64**, 1523–1534, <https://doi.org/10.1007/s10620-018-5424-6>
- 30 Liu, J.W., Li, H., Shen, S.X., Sun, L.P., Yuan, Y. and Xing, C.Z. (2018) Alternative splicing events implicated in carcinogenesis and prognosis of colorectal cancer. *J. Cancer* **9**, 1754–1764, <https://doi.org/10.7150/jca.24569>
- 31 Jeun, M., Lee, H.J., Park, S., Do, E.J., Choi, J., Sung, Y.N. et al. (2019) A novel blood-based colorectal cancer diagnostic technology using electrical detection of colon cancer secreted protein-2. *Adv. Sci.* **6**, 1802115
- 32 Dueland, S., Foss, A., Solheim, J.M., Hagness, M. and Line, P.D. (2018) Survival following liver transplantation for liver-only colorectal metastases compared with hepatocellular carcinoma. *Br. J. Surg.* **105**, 736–742, <https://doi.org/10.1002/bjs.10769>
- 33 Bauer, K.M., Watts, T.N., Buechler, S. and Hummon, A.B. (2014) Proteomic and functional investigation of the colon cancer relapse-associated genes NOX4 and ITGA3. *J. Proteome Res.* **13**, 4910–4918, <https://doi.org/10.1021/pr500557n>
- 34 Gorbenko, O., Panayotou, G., Zhyvoloup, A., Volkova, D., Gout, I. and Filonenko, V. (2010) Identification of novel PTEN-binding partners: PTEN interaction with fatty acid binding protein FABP4. *Mol. Cell. Biochem.* **337**, 299–305, <https://doi.org/10.1007/s11010-009-0312-1>
- 35 Inamura, K., Song, M., Jung, S., Nishihara, R., Yamauchi, M., Lochhead, P. et al. (2016) Prediagnosis plasma adiponectin in relation to colorectal cancer risk according to KRAS mutation status. *J. Natl. Cancer Inst.* **108**, djv363, <https://doi.org/10.1093/jnci/djv363>
- 36 Liu, X., Liu, X., Qiao, T. and Chen, W. (2020) Identification of crucial genes and pathways associated with colorectal cancer by bioinformatics analysis. *Oncol. Lett.* **19**, 1881–1889
- 37 Dudgeon, C., Wang, P., Sun, X., Peng, R., Sun, Q., Yu, J. et al. (2010) PUMA induction by FoxO3a mediates the anticancer activities of the broad-range kinase inhibitor UCN-01. *Mol. Cancer Ther.* **9**, 2893–2902, <https://doi.org/10.1158/1535-7163.MCT-10-0635>
- 38 Vinuesa, A.G., Sancho, R., García-Limones, C., Behrens, A., ten Dijke, P., Calzado, M.A. et al. (2012) Vanilloid receptor-1 regulates neurogenic inflammation in colon and protects mice from colon cancer. *Cancer Res.* **72**, 1705–1716, <https://doi.org/10.1158/0008-5472.CAN-11-3693>
- 39 Molnár, B., Galamb, O., Péterfia, B., Wichmann, B., Csabai, I., Bodor, A. et al. (2018) Gene promoter and exon DNA methylation changes in colon cancer development - mRNA expression and tumor mutation alterations. *BMC Cancer* **18**, 695, <https://doi.org/10.1186/s12885-018-4609-x>
- 40 Renfro, L.A., Goldberg, R.M., Grothey, A., Sobrero, A., Adams, R., Seymour, M.T. et al. (2017) Clinical calculator for early mortality in metastatic colorectal cancer: an analysis of patients from 28 clinical trials in the Aide et Recherche en Cancerologie Digestive Database. *J. Clin. Oncol.* **35**, 1929–1937, <https://doi.org/10.1200/JCO.2016.71.5771>
- 41 Sjoquist, K.M., Renfro, L.A., Simes, R.J., Tebbutt, N.C., Clarke, S., Seymour, M.T. et al. (2018) Personalizing survival predictions in advanced colorectal cancer: The ARCAD Nomogram Project. *J. Natl. Cancer Inst.* **110**, 638–648, <https://doi.org/10.1093/jnci/djx253>
- 42 Reichling, C., Taieb, J., Derangere, V., Klopfenstein, Q., Le Malicot, K., Gornet, J.M. et al. (2019) Artificial intelligence-guided tissue analysis combined with immune infiltrate assessment predicts stage III colon cancer outcomes in PETACC08 study. *Gut*, 681–690, <https://doi.org/10.1136/gutjnl-2019-319292>
- 43 Mo, S., Dai, W., Xiang, W., Li, Y., Feng, Y., Zhang, L. et al. (2019) Prognostic and predictive value of an autophagy-related signature for early relapse in stages I–III colon cancer. *Carcinogenesis* **40**, 861–870, <https://doi.org/10.1093/carcin/bgz031>
- 44 Drew, J.E. (2012) Molecular mechanisms linking adipokines to obesity-related colon cancer: focus on leptin. *Proc. Nutr. Soc.* **71**, 175–180, <https://doi.org/10.1017/S0029665111003259>
- 45 Mørch, L.S., Lidegaard, Ø., Keiding, N., Løkkegaard, E. and Kjær, S.K. (2016) The influence of hormone therapies on colon and rectal cancer. *Eur. J. Epidemiol.* **31**, 481–489, <https://doi.org/10.1007/s10654-016-0116-z>
- 46 Wen, Y.A., Xiong, X., Zaytseva, Y.Y., Napier, D.L., Vallee, E., Li, A.T. et al. (2018) Downregulation of SREBP inhibits tumor growth and initiation by altering cellular metabolism in colon cancer. *Cell Death Dis.* **9**, 265, <https://doi.org/10.1038/s41419-018-0330-6>
- 47 Huang, Q.R. and Pan, X.B. (2019) Prognostic lncRNAs, miRNAs, and mRNAs form a competing endogenous RNA network in colon cancer. *Front. Oncol.* **9**, 712, <https://doi.org/10.3389/fonc.2019.00712>
- 48 Yang, H., Lin, H.C., Liu, H., Gan, D., Jin, W., Cui, C. et al. (2020) A 6 lncRNA-based risk score system for predicting the recurrence of colon adenocarcinoma patients. *Front. Oncol.* **10**, 81, <https://doi.org/10.3389/fonc.2020.00081>
- 49 Kim, H.S., Kim, K.M., Lee, S.B., Kim, G.R., Han, Y.D., Cho, M.S. et al. (2019) Clinicopathological and biomolecular characteristics of stage IIB/IIC and stage IIIA colon cancer: insight into the survival paradox. *J. Surg. Oncol.* **120**, 423–430, <https://doi.org/10.1002/jso.25515>
- 50 Lin, R., Zhang, H., Yuan, Y., He, Q., Zhou, J., Li, S. et al. (2020) Fatty acid oxidation controls CD8(+) tissue-resident memory T-cell survival in gastric adenocarcinoma. *Cancer Immunol. Res.* **8**, 479–492
- 51 Dandawate, P., Subramaniam, D., Panovich, P., Standing, D., Krishnamachary, B., Kaushik, G. et al. (2020) Cucurbitacin B and I inhibits colon cancer growth by targeting the Notch signaling pathway. *Sci. Rep.* **10**, 1290, <https://doi.org/10.1038/s41598-020-57940-9>

	pvalue	Hazard ratio
SLC10A2	0.008	1.833(1.174–2.860)
CXCL3	0.007	0.976(0.959–0.993)
NOX4	0.009	1.603(1.126–2.283)
FABP4	<0.001	1.014(1.007–1.020)
ADIPOQ	<0.001	1.102(1.047–1.160)
CCL19	0.006	1.030(1.008–1.051)
PLCG2	0.003	1.676(1.192–2.355)
IGHG1	<0.001	1.001(1.000–1.001)
IGHG4	0.008	1.000(1.000–1.001)
IGHV4–31	0.008	1.008(1.002–1.014)
IGHV5–51	0.002	1.002(1.001–1.003)
IGKV1–33	0.002	1.030(1.011–1.050)
IGKV1–8	0.002	1.044(1.015–1.073)
IGLV6–57	0.003	1.002(1.001–1.003)
SEMA3G	<0.001	1.294(1.124–1.491)
INHBA	<0.001	1.054(1.022–1.086)
STC1	0.007	1.078(1.020–1.139)
UCN	0.003	1.386(1.120–1.715)
VIP	0.002	1.058(1.021–1.096)
NGFR	<0.001	1.201(1.092–1.320)
NPR1	0.004	1.504(1.136–1.991)
OXTR	<0.001	1.421(1.171–1.724)
PTH1R	<0.001	1.628(1.220–2.173)
TRDC	0.009	1.148(1.035–1.273)

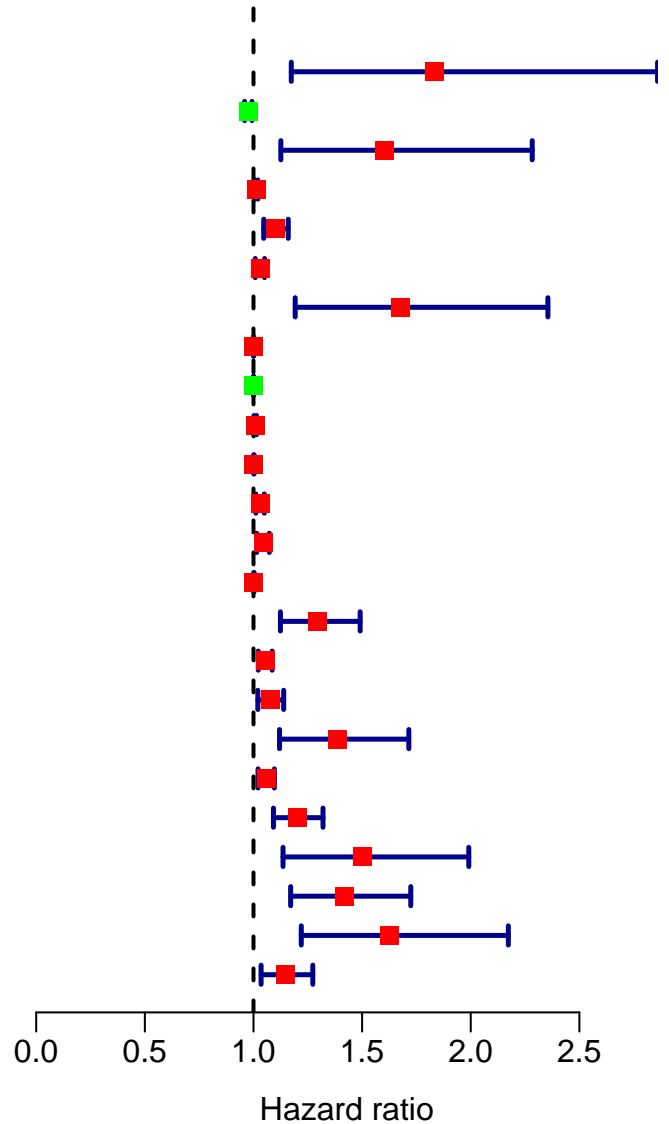


Figure S1. The hazard ratios (HR), 95% confidence intervals (CI) calculated by univariate Cox regression.

Coefficients

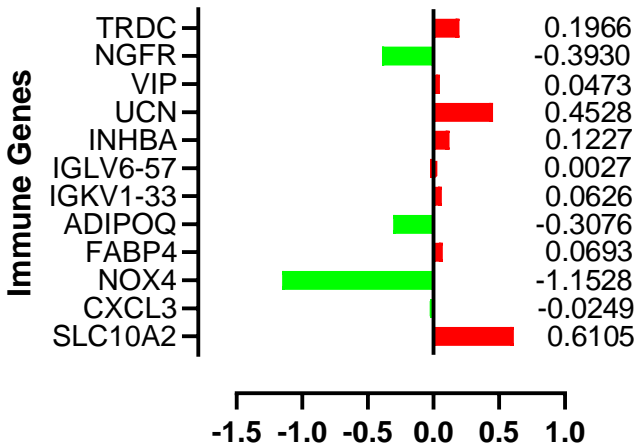
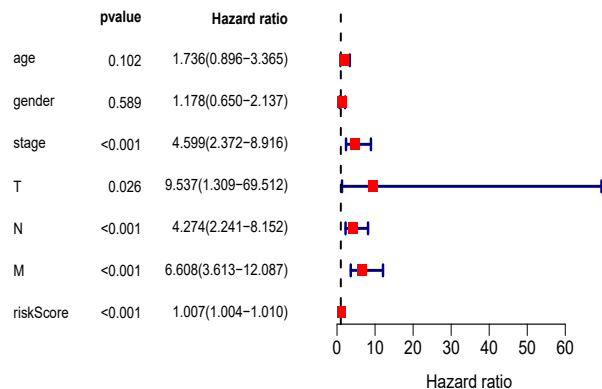
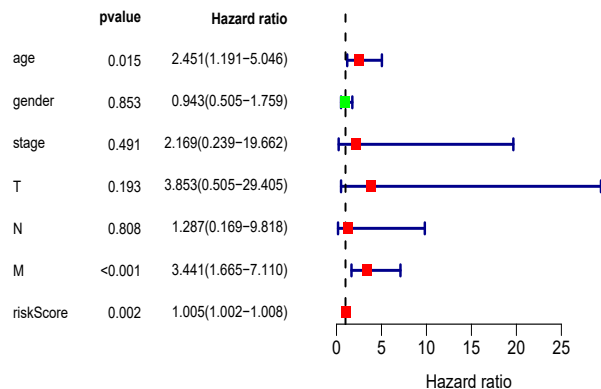


Figure S2. The coefficient of PRIGs.

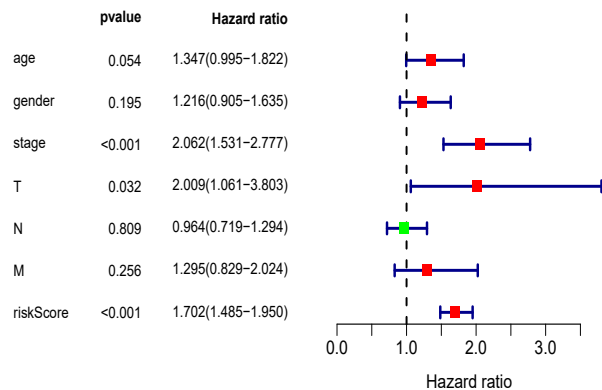
A TCGA-Univariate analysis



B TCGA-Multivariate analysis



C GEO-Univariate analysis



D GEO-Multivariate analysis

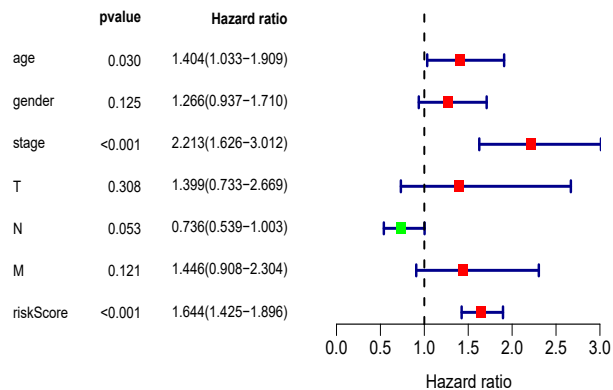


Figure S3. Prognosis model of immune genes. (A, C) Univariate Cox regression analysis. Forest plot of the association between risk factors and survival of TCGA-COAD (A) and GEO-COAD (C). (B, D) Multivariate Cox regression analysis. The risk score was an independent prognostic element in TCGA-COAD (B) and GEO-COAD (D).

Table S1. Characteristics of training and test group.

		TCGA (Training group)	GEO (Test group)
Age(years)		67.01±12.77	66.21±13.23
Gender	Female	180	262
	Male	205	325
Stage	Stage I	66	45
	Stage II	151	271
	Stage III	103	212
	Stage IV	54	56
	Unknow	11	3
T (Tumor)	T1	10	11
	T2	68	57
	T3	263	388
	T4	44	108
	Tis	1	3
	Unknow	0	20
	N0	231	317
N (Lymph Node)	N1	88	141
	N2	66	99
	N3	0	5
	NX	0	25
M (Metastasis)	M0	286	508
	M1	54	57
	Mx	40	3
	Unknow	5	19

Table S2. Prognosis-related immune genes (univariate Cox regression analysis)

PRIGs	HR	HR.95L	HR.95H	P value
CXCL3	0.976274178	0.959433832	0.993410111	0.006836376
IGHG4	1.000462714	1.000118581	1.000806966	0.008401804
IGHG1	1.000557152	1.000229499	1.000884911	0.000858607
IGHV5-51	1.00161858	1.00058123	1.002657006	0.00222059
IGLV6-57	1.00196457	1.000646266	1.003284611	0.003480915
IGHV4-31	1.008180525	1.002111576	1.014286228	0.008176801
FABP4	1.013514986	1.006982636	1.020089712	4.72E-05
CCL19	1.029586494	1.008468596	1.051146613	0.005824639
IGKV1-33	1.030336759	1.011010023	1.05003295	0.001979212
IGKV1-8	1.043893862	1.015268705	1.073326095	0.002460688
INHBA	1.053507046	1.022173509	1.085801076	0.000715416
VIP	1.057597466	1.020679968	1.095850251	0.002007728
STC1	1.077990496	1.020432945	1.138794584	0.007308441
ADIPOQ	1.101937111	1.046564847	1.160239044	0.000224086
TRDC	1.148292064	1.035438282	1.273445928	0.008799448
NGFR	1.200503367	1.092020089	1.319763572	0.000155797
SEMA3G	1.294274954	1.123577659	1.490905097	0.000350682
UCN	1.386191418	1.120402289	1.715032777	0.002640879
OXTR	1.420766913	1.170702262	1.72424594	0.000377164
NPR1	1.504102806	1.13612177	1.991270048	0.004351938
NOX4	1.603287544	1.126141305	2.282600714	0.008816796
PTH1R	1.628067123	1.219526757	2.173468145	0.000945574
PLCG2	1.675520381	1.192276181	2.354629398	0.002949259
SLC10A2	1.832753743	1.174436133	2.860084245	0.007628351